

# Large-scale Oscillation of Structure-Related DNA Sequence Features in Human Chromosome 21

Wentian Li\*

*The Robert S. Boas Center for Genomics and Human Genetics, Feinstein Institute for Medical Research, North Shore LIJ Health System, 350 Community Drive, Manhasset, NY, USA.*

Pedro Miramontes†

*Departamento de Matemáticas, Facultad de Ciencias, Universidad Nacional Autónoma de México, Circuito Exterior, Ciudad Universitaria, 04510 México, D.F. and  
Departamento de Matemáticas, Universidad de Sonora, Encinas y Rosales, Hermosillo 83000 Sonora, México.*

Human chromosome 21 is the only chromosome in human genome that exhibits oscillation of (G+C)-content of cycle length of hundreds kilobases (500 kb near the right telomere). We aim at establishing the existence of similar periodicity in structure-related sequence features in order to relate this (G+C)% oscillation to other biological phenomena. The following quantities are shown to oscillate with the same 500kb periodicity in human chromosome 21: binding energy calculated by two sets of dinucleotide-based thermodynamic parameters, AA/TT and AAA/TTT bi-/tri-nucleotide density, 5'-TA-3' dinucleotide density, and signal for 10/11-base periodicity of AA/TT or AAA/TTT. These intrinsic quantities are related to structural features of the double helix of DNA molecules, such as base-pair binding, untwisting/unwinding, stiffness, and a putative tendency for nucleosome formation.

PACS numbers: 87.10.+e, 87.14.Gg, 87.15.Cc, 02.50.-r, , 02.50.Tt, 89.75Da, 89.75.Fb, 05.40.-a

## I. INTRODUCTION

DNA sequences are full of features at small, intermediate, and large scales [1]. At short distances, there is strong periodicity-of-three-nucleotide signal in protein-coding regions (but absent in non-coding regions) [2], and a weaker but ubiquitous 10-11 bases signal in many genomes [3]. At intermediate length scale, there are *Alu* sequences of about 300 bases long [4], and nucleosome-forming sequence of around 120-200 bases [5]. At large length scales, the most well known features are the existence of alternating (G+C)%-high and (G+C)%-low “isochores” [6], and the distribution of sine wave that prefers long-wavelength signals (the so-called “1/f” spectra when viewed in the spectral space [7]).

A recent survey of (G+C)% fluctuation in all human (*Homo sapiens*) chromosomes revealed that chromosome 21 exhibits a unique 500 kilobases (kb) oscillation in (G+C)% [8]. This oscillation starts around the position of 43.5 million bases (Mb) and lasts five cycles (with five (G+C)%-low six (G+C)%-high peaks). No other human chromosomes exhibit similar periodicities with such a long cycle length.

Human chromosome 21 has other special properties as compared to the rest of the human chromosomes. First, it is the shortest human chromosome. Second, its (G+C)% increases stepwise from left (centromeric) to right (telomeric, i.e., close to the end of the chromo-

some), with three distinct “super” isochore regions (see, e.g. Fig.3 of [6](b)). The 500kb oscillation of (G+C)% described above appears in the third region with the highest (G+C)% and the highest gene content. Third, the failure rate in segregating homologous chromosomes during meiosis is the highest among surviving infants in human chromosome 21 than any other human chromosomes. When this happens, the surviving infants typically carries three copies of chromosome 21 (“trisomy 21”) instead of one copy [9]. The resulting Down syndrome is the leading case of birth defects [10].

The uniqueness of the 500kb oscillation in (G+C)% in human chromosome 21 and highest trisomy rate in chromosome 21 among surviving infants motivated us to speculate the possibility that this 500kb oscillation might be somewhat related to the trisomy risk. An argument is that the periodicity in (G+C)% is a basis for certain structural periodicity, which in turn might interfere with the proper segregation of chromatids during meiosis. One intriguing observation is that for younger mothers with trisomy 21, the placement of meiosis exchange tends to be telomeric [11].

In this paper, we examine whether sequence-based structure features oscillates with the 500kb cycle length in the telomeric region of human chromosome 21. The structural features we focus on include helix binding energy, flexibility or stiffness in secondary structure of DNA helix, tendency for nucleosome formation based on periodicity of 10-11 bases, and a tendency for anchoring DNA loops.

Note that only the intrinsic quantities are calculable here: chromatin structures that depend on extrinsic protein factors require experimental data, and these

\*Electronic address: wli@nslj-genetics.org

†Electronic address: pmv@ciencias.unam.mx

5' / 3'	G	A	T	C
G	2.75/1.84	1.41/1.30	1.13/1.44	2.82/2.24
A	(see CT)	1.66/1.00	1.19/0.88	(see GT)
T	(see CA)	0.76/0.58	(see AA)	(see GA)
C	3.28/2.17	1.80/1.45	1.35/1.28	(see GG)

TABLE I: Free energy ( $\Delta G$ ) of helix binding in nearest neighbor models at 37°C with Breslauer/SantaLucia parameters (kcal/mol).

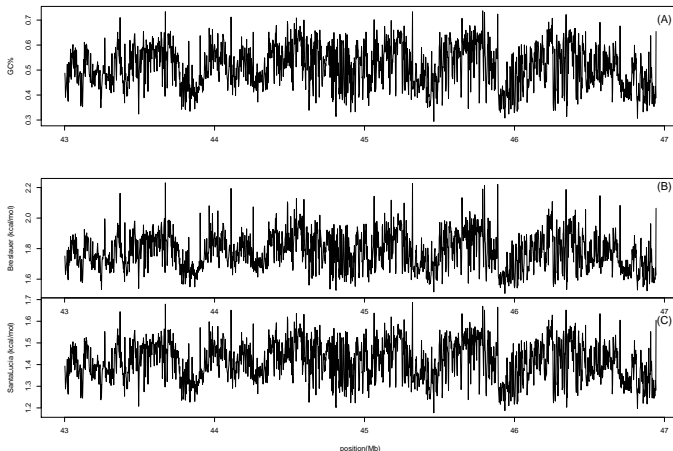


FIG. 1: (A) (G+C)% calculated in non-overlapping windows of size 2kb; (B) free energy  $\Delta G$  in nearest neighbor model with Breslauer's parameter values; (C) free energy  $\Delta G$  in nearest neighbor model with SantaLucia's parameter values; The  $x$ -axis is the chromosome position, in Mb.

evidences are not yet conclusive. Also note that the sequence-to-structure connections in some model are based on simplified assumptions, and our calculation may only give a partial picture of DNA helix structure properties. Our hope is for this work to contribute to the eventual establishment of a sequence-function connection.

## II. DNA BINDING ENERGY AND STABILITY

It has been well known that basepairs with strong bases (G-C) are more stable than basepairs with weak bases (A-T), due to the presence of three versus two hydrogen bonds. This single-base model of binding energy has been extended to dinucleotide models where a dinucleotide step (two neighboring basepairs) contributes an amount to the total binding energy [12]. There are two commonly used parameter value sets in the dinucleotide model: one by Breslauer and his colleagues [13] and another summarized by SantaLucia, also known as the unified parameters [14]. The nearest-neighbor free energy  $\Delta G$  parameter values at 37°C are listed in Table I for all 16 dinucleotide steps.

A 3.9Mb sequence from the NCBI Build 35 (May'2004, hg17) of human chromosome 21 is downloaded from the UCSC genome browser [15], starting from the po-

sition 43Mb and ending at the right telomere, of position 46.944323Mb.

Figure 1 shows the (G+C)% and averaged binding free energy  $\Delta G$  calculated by the dinucleotide model with Breslauer's and SantaLucia's parameters, using non-overlapping windows of 2kb. It is clear that binding energy is higher in (G+C)%-high peak regions, thus also oscillates with the 500kb periodicity. However, the magnitude of oscillation is larger in the free energy based on Breslauer's parameters than that using SantaLucia's parameters (range of (1.51-2.23) versus (1.18-1.69)).

Among the values of  $\Delta G$  in Table I, the highest helix binding energies are usually associated with two strong bases (G or C), with the exception of 1.84 kcal/mol for GG/CC dinucleotide in SantaLucia's parameters. The lowest binding energies tend to be associated with two weak bases (A or T), but with the exceptions of AA/TT (1.66 kcal/mol) and AT (1.19 kcal/mol) dinucleotides in Breslauer's parameters. The difference between the two sets of parameters is the largest for CG (1.11 kcal/mol, 40.7% of the average between the two parameters), GG/CC (0.91 kcal/mol, 39.7%), and AA/TT (0.66 kcal/mol, 49.6%) dinucleotides. With these exceptions, one may not automatically assume binding energy to fluctuate the same way as (G+C)%. What Figure 1 have shown is that the difference between the single-base model (counting the number of weak and strong bases) and the dinucleotide models is not large enough to destroy the 500kb oscillation in binding energy.

The correlation coefficient between windowed energy values and the (G+C)% values was calculated (the first two lines in Table II). These correlation values show that SantaLucia parameters are more correlated with the GC% than Breslauer's parameters (correlation coefficient of 0.998 versus 0.981 using the 2kb window). By examining the two sets of free energy parameters in Table I closely, it is clear that difference can be traced to the fact that Breslauer's parameters assign a higher energy value for two AT-rich dinucleotides than SantaLucia's parameters: 5'-AA-3' and 5'-AT-3'. It is still debatable whether Breslauer's or SantaLucia's parameters reflect the *in vivo* situation of helix local thermodynamics [16], and the issue may not be settled soon [17].

## III. DNA FLEXIBILITY, STIFFNESS, AND UNTWISTING

Without an actual measurement of the DNA polymer mechanic properties, we rely on dinucleotides and trinucleotides that are known to be related to the DNA flexibility, stiffness, and untwisting to study the variation of these properties along the chromosome. For example, the AA..A/TT..T tract is known to have a stiff configuration because of an additional hydrogen bond between adjacent pairs along two diagonally located bases [18]. This hypothesis had been confirmed for AA/TT dinucleotide by their limited range of roll and slide values [19]. We use

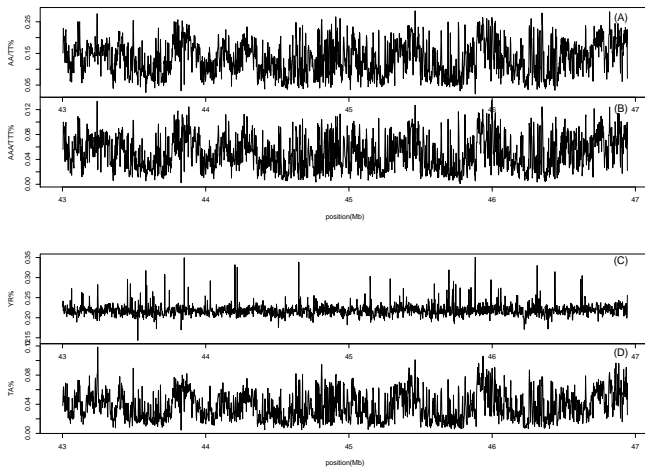


FIG. 2: (A): Density of AA/TT in non-overlapping windows of size 2kb; (B) AAA/TTT density; (C) 5'-YR-3' density; (D) 5'-TA-3' density.

AA/TT dinucleotide and AAA/TTT trinucleotide density in a moving window as an indicator for the intrinsic stiffness of the double helix.

Unlike A/T-tracts, 5'-pyrimidine-purine-3' (5'-YR-3') steps can adopt two possible configurations, and thus they are flexible [20]. In a simplified approach, we use 5'-YR-3' density as an indicator for flexibility of the DNA double helix.

Among the four 5'-YR-3' steps (CA, CG, TA, TG), 5'-TA-3' has the weakest basepair binding. The biconfiguration nature and weak binding make 5'-TA-3' one of the best candidates for untwisting initiation sites of double helix [20]. We use the 5'-YR-3' and 5'-TA-3' density in moving windows as an indicator for an untwisting potential.

Figure 2 shows densities of the above mentioned di-/tri-nucleotide: AA/TT%, AAA/TTT %, 5'-YR-3' %, and 5'-TA-3' %. The 500kb oscillation in the first two densities is clearly seen. The 5'-YR-3' density does not exhibit any regular oscillation of 500kb, whereas 5'-TA-3' density does oscillate with the 500kb wavelength.

Note that the signal we are measuring by the di-/tri-nucleotide density is different from that of CpG island [21]. In detecting CpG islands, the density of 5'-CG-3' dinucleotide is normalized by the square of GC% (the observed over expected, or O/E), and the presence of a signal require the 5'-CG-3' density to be at least a quadratic function of GC%. In fact, it was known that the O/E signal increases with the GC%, indicating a cubic relationship between 5'-CG-3' density and GC% in CpG islands [22]. Here only the “linear” signal was measured.

#### IV. PERIODICITY-10-BASE SIGNAL AND NUCLEOSOME FORMING POTENTIAL

It has been known that almost all genomes contain a AA-10b-AA/TT-10b-TT signal [3], where the “10b” can

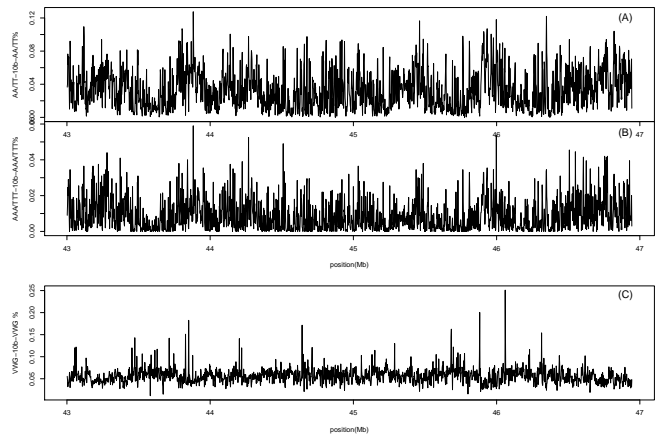


FIG. 3: (A) Density of AA-10b-AA/TT-10b-TT in non-overlapping window of size 2kb; (B) AAA-10b-AAA/TTT-10b-TTT density. (C) VWG-10b-VWG density, where VWG indicates [not-T][A/T][G] or it's reverse complement triplet [C][A/T][not-A].

be 10 or 11 bases for individual cases, but after averaging becomes a real number between 10 and 11. This periodic signal is also present in the aligned nucleosome-forming sequences [23]. We count the number of occurrence of AA-10-AA, TT-10-TT, AA-11-AA, and TT-11-TT in a moving window, then convert to density (similar calculation for AAA-10b-AAA/TTT-10b-TTT density is also carried out). As a crude approximation, this density is used to indicate the region's tendency for nucleosome formation.

Figure 3 (A)(B) show the AA-10b-AA/TT-10b-TT and AAA-10b-AAA/TTT-10b-TTT density in a 2kb non-overlapping moving window. The 500kb oscillation is clearly seen, and may support the idea that the nucleosome forming strength also oscillates with that wavelength in this region.

However, it was suggested that the regular spacing of 10 bases of another triplet motif, [not-T][A/T][G], can be considered as a nucleosome formation signal (called “VWG” signal) [24]. We count the occurrence of [not-T][A/T][G]-10/11-[not-T][A/T][G] and [C][A/T][not-A]-10/11-[C][A/T][not-A] in a moving window, whose density is plotted in Figure 3(C). This VWG signal does not exhibit a 500kb oscillation in this region.

In a more sophisticated study based on discriminant analysis, a composite measure called “nucleosome formation potential” (NFP) was proposed [25]. As shown in Fig.1 of [26], this NFP value decreases with GC%. Since AA-10b-AA/TT-10b-TT and AAA-10b-AAA/TTT-10b-TTT density also decreases with GC%, the two measures are consistent. The VWG signal, however, does not have a simple relationship with GC%, though mostly it increases with GC%. Whether one can predict nucleosome forming potential of a DNA sequence accurately, and whether such an intrinsic potential really exists, seems still to be open questions, and it is possible that either AA/TT-10b-AA/TT or VWG-10b-VWG signal does not

present the whole picture on nucleosome formation.

## V. DISCUSSION AND CONCLUSION

Besides the helix structure related intrinsic features, the scaffold/matrix-attached-regions (S/MARs) is another pattern that can be determined from the DNA sequence. S/MARs are the base/foundation of DNA loops [27], and S/MAR sequences can be obtained from S/MAR databases such as the one developed at the University of Göttingen [28].

By examining the top 34 most frequent hexamers in S/MAR sequences (Table 2 of [28](b)), it is clear that S/MARs are AT-rich [29]. In fact, only 11 hexamers contain one G or C, ranked 10, 16–18, 21, 22, 25–27, 29, 30 in the top34, and the rest consist exclusively of A and T [28]. It is not surprising that S/MAR hexamer density (percentage of hexamers that match the top 34 most frequent S/MAR hexamer motifs and their reverse complement) also oscillates with a 500kb wavelenegth in this region [30].

The existence of 500kb oscillation in most of the quantities we have examined indicates that these structure-related sequence features are correlated with GC%. To assess this correlation directly, Figure 4 shows the scatter plot of ten quantities used in Figures 1-3 as versus GC%, and Table II lists correlation coefficients of all pairs among these eleven quantities. Figure 4 and Table II have confirmed that these structure-based sequence features are highly correlated (test results of these correlation coefficients are all significant with the exception of a few pairs involving 5'-YR-3'), and GC% can be used as a good surrogate for these features (with the exception of 5'-YR-3').

Density of 5'-YR-'3 is not correlated with other quantities studied (4 correlation coefficients are not significant at the  $p$ -value=0.01 level, and 5 other correlation coefficients, though significant, are rather weak). The next group of quantities that have weak correlation with others are the AAA-10b-AAA/TTT-10b-TTT and VWG-10b-VWG densities, with several correlation coefficients in the 0.4-0.5 range.

One may ask the question on whether the correlation between these quantities and GC% is "trivial", because these patterns are either dominated by GC-rich or AT-rich di- tri-nucleotides. This question can be addressed by examining the GC%-preserving random sequences. In Figure 4 the ten structure-related quantities for the random sequences are shown as a function of GC% (circles). Several interesting observations can be made.

- Binding energies calculated on real DNA sequences are very close to those calculated on randomized sequences. However, the binding energy of real DNA sequences is slightly lower than that of random sequences at high GC% values. A similar observation was made in [31] (Fig.1(C) of [31]) on the "relative" thermostability.

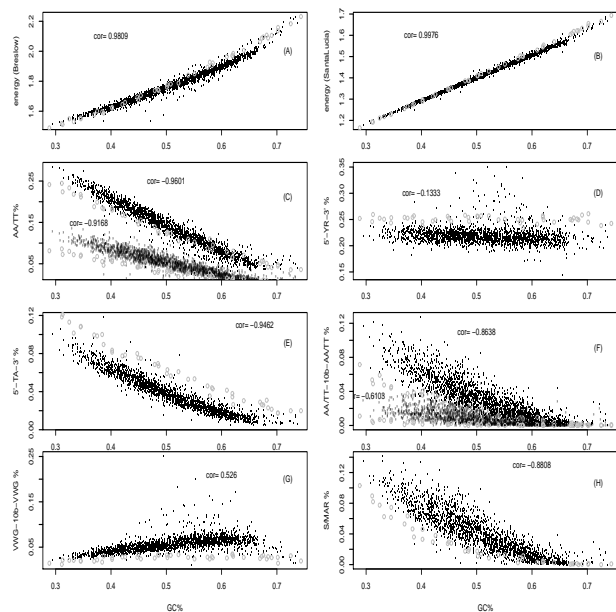


FIG. 4: Scatter plots of ten quantities versus GC%: (A) helix binding energy by Breslaue’s model; (B) binding energy by SantaLucia’s model; (C) AA/TT (upper) and AAA/TTT (lower, using the symbol ’) densities; (D) 5'-YR-3' density; (E) 5'-TA-3' densities; (F) AA-10b-AA/TT-10b-TT (upper) and AAA-10b-AAA/TTT-10b-TTT (lower, using the symbol ’) densities; (G) VWG-10-VWG densities; and (H) density of the top 34 hexamers in known S/MAR sequences and their reverse complements. The corresponding values for randomized sequences are also shown (grey circles). The correlation coefficient between these quantities andf GC% is indicated on the plot.

- The A/T-tract density is higher in real DNA sequences than randomized sequences, mainly in the AT-rich ranges. It indicates that DNA sequences are more rigid than randomized sequences in general.
- The biconfigurational 5'-YR-3' dinucleotide density is lower in real DNA sequences than randomized sequences (with some exceptions for DNA segments with GC% around 50%-60%). It indicates DNA sequences are less flexible than randomized sequences.
- The 5'-TA-3' density is lower in DNA sequences than random sequences, making them less susceptible for helix untwistings.
- The periodicity of 10/11 bp signal for both AA/TT, AAA/TTT, and VWG triplet has a stronger presence in real DNA sequences than random sequences, probably making them more likely to form nucleosomes.
- The S/MAR potential is higher in DNA sequences than randomized sequences.

	GC	Breslauer	SantaLucia	5'YR3'	AA	AAA	5'TA3'	AA10AA	AAA10AAA	VWG10VWG
Breslauer	0.981									
SantaLucia	0.998	0.985								
5'YR3'	-0.133	-0.195	-0.103							
AA	-0.960	-0.896	-0.950	-0.042*						
AAA	-0.917	-0.844	-0.903	-0.044*	0.974					
5'TA3'	-0.946	-0.915	-0.947	0.183	0.912	0.858				
AA10AA	-0.864	-0.791	-0.851	-0.043*	0.922	0.956	0.810			
AAA10AAA	-0.610	-0.545	-0.595	-0.064	0.683	0.789	0.557	0.866		
VWG10VWG	0.526	0.398	0.514	0.279	-0.657	-0.637	-0.574	-0.601	-0.458	
S/MAR	-0.881	-0.807	-0.868	-0.002*	0.929	0.967	0.854	0.947	0.810	-0.617

TABLE II: Correlation coefficients of eleven quantities obtained from non-overlapping 2kb windows: GC%, binding energy by Breslauer’s model and SantaLucia’s model, densities of 5'-YR-3', AA/TT, AAA/TTT, 5'-TA-3', AA-10b-AA/TT-10b-TT, AAA-10b-AAA/TTT-10b-TTT, VWG-10b-VWG, and density of top S/MAR hexamers. Testing of correlation coefficient equal to zero is significant at  $p$ -value=0.01 level for all pairs except those marked by the stars (YR-AA  $p$ =0.064, YR-AAA  $p$ =0.049, YR-AA10AA  $p$ =0.056, and YR-SMAR  $p$ =0.93).

From these observations, one may expect that the binding energy faithfully follows the same variation and oscillation as GC%; A/T tract density, TA density, AAA-10b-AAA signal, and S/MAR signal more or less follow the same oscillation as GC%; YR density, AAA-10b-AAA signal, and YWG-10b-YWG signal may not follow the same oscillation as GC%.

It has been known that GC% conveys biological information [6](c). For example, the Giemsa-dark chromosome staining band, or G-band, is AT-rich, whereas the Giemsa-light band or R-band is GC-rich [32], or by a new hypothesis, AT-rich and GC-rich relative to its neighboring bands [33]. Gene density is another example, with GC-rich regions being relatively gene-rich [34]. Fluorescence microscopy images show that chromosomes inside the nucleus are organized in a radial order, called “chromosome territories” [35]. The GC-rich, gene-rich regions tend to be located towards the center of the nucleus [36], and the corresponding chromatin compartments are more “open” [35].

Without experimental evidences, it is difficult to speculate what type of high-order chromatin structure this 500kb oscillation might cause. According to the chromatin structure model summarized in [37], there could be multiple level of foldings in the hierarchical structure of a chromatid: Watson-Crick’s double helix (10bp for one helix turn), nucleosomes ( $\sim 200$ bp per unit), solenoids (6 nucleosome units per helix turn, or 1.2kb) that twist to form a loop of  $\sim 50$ kb, rosettes that consist of 6 loops ( $\sim 300$  kb), coils that consist of 30 rosettes ( $\sim 9$ Mb), and finally the chromatids consist of, for a medium sized human chromosome,  $\sim 10$  coils. Within the framework of this model, our 500kb oscillation matches roughly the size of a rosette. However, we should caution that the exact figure for the size of these hierarchical units is illustrative, and the model itself may be too much based on *in vitro* experiments, and on inactive cells [38].

The unique large-scale oscillation of GC% in human chromosome 21 studied in this paper and in [8] can be

further analyzed from several perspectives. One is about its evolutionary presevation in other species. Due to the high degree of similarity between human and chimpanzee, it is natural to assume that the same 500kb oscillation would also be present in chimpanzee genome. Indeed, it was shown that 500kb oscillation exists in chimpanzee chromosome 22 [30]. On the other hand, no such 500kb oscillation was observed in mouse genome. It would be interesting to check its existence in species in-between mouse and human.

It was suggested for the yeast genome [39] that the transcription direction of open reading frame (ORF) points from GC-rich to GC-poor regions. Combined with the general picture that DNA loop anchored in AT-rich regions whereas the GC-rich part of the loop is exposed to the outside, transcription likely starts from the top of DNA loop to loop base. Although the length scale between two GC-rich regions analyzed in the yeast genome ( $\sim 10$ kb) is much shorter than the GC% oscillation length studied here, there are some evidence that gene density on two opposite strands alternating in this region (Fig.5(c) of [8]). A more careful analysis is needed to confirm the similarity between human and yeast genome, and the regular oscillation of GC% discussed here provides an ideal test ground.

In conclusion, the 500kb oscillation in GC% as reported in [8] was shown to lead to similar oscillation of some intrinsic structure-related patterns. And we hypothesis that a regular oscillation in chromatin structure with the same wavelength is also present in this region.

### Acknowledgements

W.L. acknowledges the financial support at the The Robert S Boas Center for Genomics and Human Genetics. P.M. thanks the support of DGAPA project IN111003.

- 
- [1] W. Li, *Comp. & Chem.*, **21**, 257-272 (1997).
- [2] J.W. Fickett, *Nucl. Acids Res.*, **10**, 5303-5318 (1982); V.R. Chechetkin, L.A. Knizhnikova, A.Y. Turygin, *J. Biomol. Struct. Dyn.*, **12**, 271-299 (1994); G. Gutierrez and A. Marin, *J. Theo. Biol.*, **167**, 413-414 (1994); S. Tiwari, S. Ramachandran, A. Bhattacharya, S. Bhattacharya, R. Ramaswamy, *Comp Appl. Biosc.*, **13**, 263-270 (1997); W. Lee and L. Luo, *Phys. Rev. E*, **56**, 848-851 (1997).
- [3] E.N. Trifonov and J.L. Sussman, *Proc. Natl. Acad. Sci. USA*, **77**, 3816-3820 (1980); J. Widom, *J. Mol. Biol.*, **259**, 579-588 (1996); V.R. Chechetkin and V.V. Lobzin, *J. Biomol. Struct. Dyn.*, **15**, 937-947 (1998); H. Herzog, O. Weiss, E.N. Trifonov, *Bioinformatics*, **15**, 187-193 (1999); E. Larsabal and A. Danchin, *BMC Bioinformatics*, **6**, 206 (2005).
- [4] C.W. Schmid and W.R. Jelenik WR, *Science*, **216**, 1065-1070 (1982); C. Willard, H.T. Nguyen, C.W. Schmid, *J. Mol. Evo.*, **26**, 180-186 (1987); M.A. Batzer and P.L. Deininger, *Nature Rev. Genet.*, **3**, 370-379 (2002).
- [5] D. Hewish and L. Burgoyne, *Bioch. Biophys. Res. Comm.*, **52**, 504-510 (1973); H.R. Widlund, et al., *J. Mol. Biol.*, **267**, 807-817 (1997); J. Widom, *Q. Rev. Biophys.*, **34**, 269-324 (2001).
- [6] (a) G. Macaya, J.P. Thiery, G. Bernardi, *J. Mol. Biol.*, **108**, 237-254 (1976); (b) G. Bernardi, *Gene*, **276**, 3-13 (2001); (c) G. Bernardi, *Structural and Evolutionary Genomics* (Elsevier, 2004).
- [7] W. Li and K. Kaneko, *Europhys. Lett.*, **17**, 655-660 (1992); R.F. Voss, *Phys. Rev. Letts.*, **68**, 3805-3808 (1992); X. Lu, Z. Sun, H. Chen, Y. Li, *Phys. Rev. E*, **58**, 3578-3584 (1998); A. Fukushima, et al., *Gene*, **300**, 203-211 (2002); W. Li and D. Holste, *Fluct. Noise Letts.*, **4**, L453-L464; W. Li and D. Holste, *Phys. Rev. E*, **71**, 041910 (2005).
- [8] W. Li and D. Holste, *Comput. Biol. and Chem.*, **28**, 393-399 (2004).
- [9] T. Hassold and P. Hunt, *Nature Rev. Genet.*, **2**, 280-291 (2001).
- [10] S.E. Antonarakis, et al., *Nature Rev. Genet.*, **5**, 725-738 (2004); D. Patterson and A.C.S. Costa, *ibid.*, **6**, 137-147 (2005).
- [11] N.E. Lamb, et al., *Am. J. Hum. Genet.*, **76**, 91-99 (2005).
- [12] H. DeVoe and I. Tinoco Jr., *J. Mol. Biol.*, **4**, 500-517 (1962).
- [13] K.J. Breslauer, R. Frank, H. Blöcker, L.A. Marky, *Proc. Natl. Acad. Sci. USA*, **83**, 3746-3750 (1986).
- [14] J. SantaLucia Jr., *Proc. Natl. Acad. Sci.*, **95**, 1460-1465 (1998).
- [15] Genome browser from the University of California at Santa Cruz (UCSC) Genome Bioinformatics Site. URL: <http://genome.ucsc.edu/>.
- [16] P. Miramontes and G. Cocho, *Physica A*, **321**, 577-586 (2003).
- [17] A. Panjkovich and F. Melo, *Bioinformatics*, **21**, 711-722 (2005).
- [18] H.C.M. Nelson, J.T. Finch, B.F. Luisi, A. Klug, *Nature*, **33**, 221-226 (1987).
- [19] M.A. El Hassan and C.R. Calladine, *Phil. Trans. Royal Soc. London A*, **355**, 43-100 (1997).
- [20] C.R. Calladine, H.R. Drew, B.F. Luisi, A.A. Travers, *Understanding DNA – The Molecule and How It Works* 3rd edition (Elsevier, 2004).
- [21] M. Gardiner-Garden and M. Frommer, *J. Mol. Biol.*, **196**, 261-282 (1987); F. Larsen, G. Gundersen, R. Lopez, H. Prydz, *Genomics*, **13**, 1095-1107 (1992).
- [22] K. Matsuo, et al., *Somatic Cell and Mol. Genet.*, **19**, 535-543 (1993).
- [23] S.C. Satchwell, H.R. Drew, A.A. Travers, *J. Mol. Biol.*, **191**, 659-675 (1986);
- [24] P. Baldi, S. Brunak, Y. Chauvin, A. Krogh, *J. Mol. Biol.*, **263**, 503-510 (1996); A. Stein and M. Bina, *Nucl. Acids Res.*, **27**, 848-853 (1999).
- [25] V.G. Levitsky, O.A. Podkolodnaya, N.A. Kolchanov, N.L. Podkolodny, *Bioinformatics*, **17**, 998-1010 (2001); *ibid.* **17**, 1062-1064.
- [26] A.E. Vinogradov, *Nucl. Acids Res.*, **33**, 559-563 (2005).
- [27] J. Mirkovitch, M.E. Mirault, U.K. Laemmli, *Cell*, **39**, 223-232 (1984).
- [28] (a) I. Liebich, J. Bode, M. Frisch, E. Wingender, *Nucl. Acids Res.*, **30**, 307-309 (2002); (b) I. Liebich, J. Bode, I. Reuter, E. Wingender, *ibid.*, **30**, 3433-3442 (2002).
- [29] Y Saitoh and U.K. Laemmli, *Cell*, **76**, 609-622 (1994).
- [30] W. Li, *Gene*, submitted (2006).
- [31] A.E. Vinogradov, *Nucl. Acids Res.*, **31**, 1838-1844 (2003).
- [32] D.E. Comings, *Ann. Rev. Genet.*, **12**, 25-46 (1978); T. Ikemura and S. Aota, *J. Mol. Biol.*, **203**, 1-13 (1988).
- [33] Y. Niimura and T. Gojobori, *Proc. Natl. Acad. Sci. USA*, **99**, 797-802 (2002).
- [34] D. Mouchiroud, et al., *Gene*, **100**, 181-187 (1991); S. Zoubak, O. Clay, G. Bernardi, *ibid.*, bf 174, 95-102 (1996).
- [35] N. Sadoni, et al., *J. Cell Biol.*, **146**, 1211-1226 (1999); T. Cremer, et al., *Critical Review in Euk. Gene Exp.*, **10**, 179-212 (2000); R.R. Williams, *Trends in Genet.*, **19**, 298-302 (2003).
- [36] S. Saccone, C. Federico, G. Bernardi, *Gene*, **300**, 169-178 (2002).
- [37] J. Filipinski, et al., *EMBO J.*, **19**, 1319-1327 (1990).
- [38] K. Van Holde and J. Zlatanova, *J. Biol. Chem.*, **270**, 8373-8376 (1995).
- [39] J. Filipinski and M. Mucha, *Gene*, **300**, 63-68; A. Marin, M. Wang, G. Gutierrez, *Gene*, **333**, 151-155.